

Supporting information

Highly efficient BODIPY-doped upconversion nanoparticles for deep-red luminescence bioimaging *in vivo*

Ti Jia, Qihong Wang, Ming Xu,* Wei Yuan, Wei Feng, and Fuyou Li*

Department of Chemistry & State Key Laboratory of Molecular Engineering of Polymers, Fudan

University, Shanghai, 200433, China.

E-mail: xuming@fudan.edu.cn, fyli@fudan.edu.cn

Contents

1. Experimental procedures

1.1. General information

1.2. Synthesis and characterization of BDMO

1.3. Preparation of BDMO-doped upconversion nanoparticles

1.4. Upconversion efficiency measurements

1.5. Cytotoxicity assay

1.6. UCL bioimaging of cells

1.7. UCL bioimaging *in vivo*

2. Supplementary figures and tables

3. Reference

1. Experimental procedures

1.1. General information

All reagents and solvents were commercially available and used without further purification apart from absolute dichloromethane (DCM) used for synthesis were obtained by distillation after reflux with calcium hydride. Thin-layer chromatography (TLC) was performed on silica gel plates (Jiangyou, Yantai). Column chromatography was performed using silica gel 100-200 mesh (Taitan, Shanghai). Glass capillary tubes were purchased from Shanghai Great Wall Scientific Instrument Store. Glassware were purchased from Beijing Synthware Glass Instrument Co., Ltd. Samples for spectrum measurements were contained in 1 cm × 1 cm quartz cuvettes (Yixing Jingke Optical Instrument Co., Ltd). The ¹H NMR spectra were recorded on a Bruker spectrometer at 400 MHz. All chemical shifts are reported in the standard δ notation of parts per million (ppm). Matrix assisted laser desorption ionization-time of flight/time of flight (MALDI-TOF/TOF) mass spectrometry was performed in an AB SCIEX 5800 spectrometer (US). UV-Vis absorption spectra were recorded on a Shimadzu 3000 spectrophotometer. Fluorescence and UCL spectra were measured on an Edinburgh FLS920 (or FS5) Luminescence Spectrometer (Edinburgh Instruments, UK). The absolute UCQY was measured by FS5 luminescence spectrometer with integrating sphere module. The image of upconversion nanoparticles was recorded on a TEM (Hitachi HT7700 Exalens, Japan). Dynamic light scattering (DLS) analysis was conducted on a dynamic light scattering detection system NANO-ZS90 (England, Malvern).

1.2. Synthesis and characterization of BDMO

1,3,5,7-tetramethyl-8-(2,4,6-trimethylphenyl)-4,4-difluoro-4-bora-3a,4a-diaza-s-indacene (BDM)

BDM was synthesized referring to literature^{1, 2} with some improvements. 2,4,6-trimethylbenzaldehyde (4.30 mmol, 637.3 mg) and 2,4-dimethylpyrrole (8.60 mmol, 1.30 g) was dissolved in treated absolute DCM (130 mL), followed by addition of trifluoroacetic acid (TFA, 0.65 mmol, 74.11 mg). The mixture was stirred at room

temperature overnight under dark and Ar atmosphere. Then the reaction was cooled to 0 °C in ice bath, 2,3-dicyano-5,6-dichlorobenzoquinone (DDQ, 4.3 mmol, 976.10 mg) was added to the reaction mixture. The reaction mixture was stirred for 1 h sequentially after the ice bath was removed. At last trimethylamine (62.35 mmol, 6.30 g) was added at 0 °C in ice bath, 10 min later, boron fluoride ethyl ether (68.80 mmol, 9.77 g) was added subsequently. After the addition, the reaction mixture was warmed to room temperature and stirred for another 2 h. After the reaction was completed, the solvent was removed under reduced pressure. The residue was diluted by DCM (90 mL) and washed with deionized water (90 mL × 3) and saturated sodium chloride solution (90 mL × 1) in sequence. The crude product was first filtered with silica gel with DCM to remove the big-polarity impurities and then purified by chromatography on silica gel (petroleum ether:dichloromethane = 2:1) to give **BDM** as red solid (933.20 mg, 59% yield). ¹H NMR (CDCl₃, 400 MHz) δ 6.95 (s, 2H), 5.96 (s, 2H), 2.56 (s, 6H), 2.33 (s, 3H), 2.09 (s, 6H), 1.38 (s, 6H); ¹³C NMR (CDCl₃, 100 MHz) δ 155.09, 142.30, 141.68, 138.56, 134.91, 131.12, 130.61, 128.98, 120.78, 21.20, 19.50, 14.62, 13.40; MS (MALDI-TOF/TOF): calc. for C₂₂H₂₅BF₂N₂ [M]⁺ 366.2079, found 366.2050.

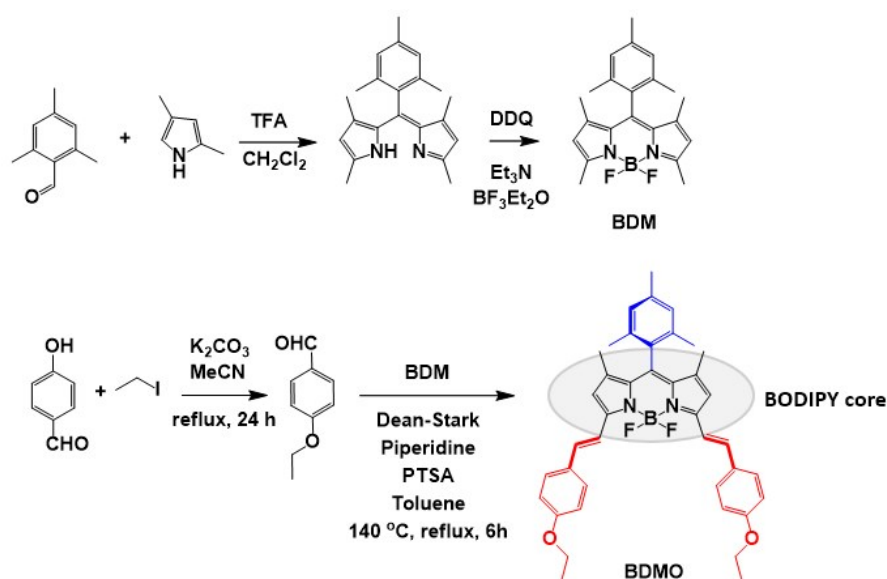
4-(ethoxy)benzaldehyde

4-(ethoxy)benzaldehyde was synthesized referring to literature.³

1,7-tetramethyl-3,5-di-[2-(4-ethoxyphenyl)ethenyl]-8-(2,4,6-trimethylphenyl)-4,4-difluoro-4-bora-3a,4a-diaza-s-indacene (BDMO)

BDMO was prepared according to the literature procedure.^{4,5} In a round bottomed flask equipped with a Dean-Stark apparatus, 4-(ethoxy)benzaldehyde (2.22 mmol, 334 mg), piperidine (1 mL) and a crystal of p-TsOH were added to a stirred solution of compound BDM (0.55 mmol, 200 mg) in 5 mL toluene. The solution was heated at its boiling point until it had evaporated to dryness. The resulting solid was washed with water three times and extracted with dichloromethane. The organic phase was dried over MgSO₄ and the solvent was evaporated under reduced pressure. The resulting crude residue was purified by column chromatography on silica by eluting with ethyl

acetate/n-hexane (1:10). ^1H NMR (CDCl_3 , 400 MHz) δ 7.64-7.60 (d, 2H), 7.58-7.55 (d, 4H), 7.22-7.18 (d, 2H), 6.96 (s, 2H), 6.93-6.91 (d, 4H), 6.60 (s, 2H), 4.11-4.06 (q, 4H), 2.35 (s, 3H), 2.12 (s, 6H), 1.46-1.42 (t, 12H); ^{13}C NMR (101 MHz, CDCl_3) δ 159.81, 152.73, 141.75, 138.03, 135.83, 135.32, 133.16, 129.41, 129.07, 129.03, 128.88, 128.56, 117.51, 117.13, 114.78, 63.59, 29.73, 14.83, 14.61. MS (MALDI-TOF/TOF): calc. for $\text{C}_{40}\text{H}_{41}\text{BF}_2\text{N}_2\text{O}_2$ $[\text{M}]^+$ 630.3229, found 630.2672.



Scheme S1 Chemical structure and synthetic route of **BDMO**.

1.3. Preparation of BDMO-doped upconversion nanoparticles

The upconversion nanoparticles were prepared according to a modified reported procedure.^{6,7} In a 25 mL of glass round bottom flask, 400 mg of Pluronic F127 and 0.5 mg of BDMO (7.9×10^{-4} mmol) were completely dissolved in toluene. The solvent was evaporated under reduced pressure and then completely removed through the oil pump. The solid residue was then dissolved under magnetic stirring with 20 mL of HCl solution (0.85 mol L^{-1}). TEOS (0.4 mL) was then added to the resulting aqueous solution followed by DMDMS (90 μL) after 6 h. The mixture was kept under stirring for 48 h at room temperature before dialysis treatments and measurements.

1.4. Upconversion efficiency measurements

The upconversion efficiency of BDMO molecules was calculated were calculated according to equation (1).⁸

$$\Phi_{\text{sample}} = \frac{N_{\text{em}}(\text{sample})}{N_{\text{ex}}(\text{blank}) - N_{\text{ex}}(\text{sample})} \quad (1)$$

N_{em} and N_{ex} represent all the number of the emitted photons and the excited photons collected by the detector through integrating sphere, respectively. The concentration of BDMO is $5 \times 10^{-6} \text{ mol L}^{-1}$.

The upconversion efficiency of the BDMO-doped upconversion nanoparticles were calculated according to equation (2).⁹

$$\Phi_{\text{sample}} = \Phi_{\text{reference}} \frac{I_{\text{sample}}}{I_{\text{reference}}} \cdot \frac{A_{\text{reference}}}{A_{\text{sample}}} \cdot \left(\frac{\eta_{\text{sample}}}{\eta_{\text{reference}}} \right)^2 \quad (2)$$

Φ_{sample} and $\Phi_{\text{reference}}$ stand for UCL quantum yield of sample upconversion nanoparticles and reference BDMO, respectively. A_{sample} and $A_{\text{reference}}$ stand for absorption of upconversion nanoparticles and BDMO, respectively. I_{sample} and $I_{\text{reference}}$ stand for integrated UCL intensity of upconversion nanoparticles and BDMO, respectively. η_{sample} and $\eta_{\text{reference}}$ stand for the refractive index of water (for upconversion nanoparticles) and reference solvent (for BDMO), respectively. The solid content of upconversion nanoparticles was $\sim 2.26\%$.

Table S1 Upconversion efficiencies (ϕ_{UC}) of BDMO molecules and BDMO-doped upconversion nanoparticles.

	Solvent	ϕ_{UC}
BDMO	DCM	16.6%
	EtOH	12.1%
BDMO-doped NPs	H ₂ O	6.9%

1.5. Cytotoxicity assay

HeLa cells were obtained from American Type Culture Collection and grown in DMEM (High glucose) medium supplemented with 10% FBS. Cells were incubated in

a 5% CO₂ humidified incubator at 37 °C and typically passaged with sub-cultivation ratio of 1:4 every two days. The cytotoxicity of upconversion nanoparticles against HeLa cells were measured by using a standard MTT assay. The cells were seeded into 96-well cell culture plate at 5×10⁴ /well in complete medium, the medium contained DMEM and 10% fetal bovine serum (FBS), the cells was incubated for 24 h at 37 °C under 5 % CO₂ to allow the cells attach. After the medium was removed and washed with PBS for three times, cells were incubated with fresh medium containing various concentrations of upconversion nanoparticles for 24 h and 48 h. The cell viability was determined by measuring the light absorbance at 490 nm with a microplate reader.

1.6. UCL bioimaging of cells

DAPI solution and Lyso-Tracker Green were from Shanghai Beyotime Biotechnology. DMEM (High glucose) medium were from Hyclone. Foetal Bovine Serum (FBS) was from Bovogen. Other biological reagents were of analytical grade and were purchased from local sources. All cell images were taken by a confocal upconversion luminescence microscopy (CUCLM) system.^{10, 11}

Raw 264.7 cells were obtained from American Type Culture Collection. The cells were seeded into the confocal petri dish in complete medium (90% DMEM and 10% FBS), and then incubated for 12 h under standard culture conditions (atmosphere of 5% CO₂ and 95% air at 37 °C) to allow cells to attach. For the UCL imaging of cells, the cells were washed three times with DMEM, and then incubated with 2 mL of FBS-free DMEM solution containing BDMO-doped nanoparticles (200 µg mL⁻¹) under standard culture conditions for 2 h. BDMO-doped nanoparticles were firstly prepared as a water solution with a concentration of 10 mg mL⁻¹ and diluted with DMEM for cell incubation. The cells were washed for three times with fresh DMEM to remove extracellular free nanoparticles and incubated with DEMA containing Lyso-Tracker Green (50 nM) for 30 min. After incubation, the cells were washed thrice and fixed with paraformaldehyde (4%) for 10 min. Then, DAPI solution was added to incubate for 5 min after washing for three times. Finally, cells were washed thrice with 2 mL of PBS, and 2 mL of PBS was added and then observed under CUCLM system (63× oil

objective) under excitation at 405 nm (DAPI), 488 nm (Lyso-Tracker Green) and 730 nm (BDMO-doped nanoparticles). Emission light at 420-450 nm (blue light channel, DAPI), 510-600 nm (green light channel, Lyso-Tracker Green), and 610-700 nm (deep red light channel, BDMO-doped nanoparticles) were collected.

1.7. UCL bioimaging *in vivo*

All animal experiments were performed in accordance with the guidelines of the Institutional Animal Care and Use Committee of Fudan University and the institutional guidelines of current international laws and polices (Guide for the Care and Use of Laboratory Animals, National Institutes of Health (NIH) Publication No. 85-23, 1985, revised 1996), as well as approved by the ethical committee of Fudan University. Balb/c female mice were purchased from Shanghai SLAC Laboratory Animal CO. LTD (Shanghai, China). Animals were maintained in our animal care facility and housed five per cage at room temperature (22 ± 2 °C) with food and water ad libitum.

The *in vivo* imaging system uses an external semiconductor laser (730 nm or 635 nm) as the excitation source and a cooled electron multiplying charge coupled device (EMCCD, Andor DU897) as the signal collector. 720 short-pass filter or band-pass filter was used.¹¹

Signal-to-noise ratio (SNR) = [(average luminous intensity of ROI 1)-(average luminous intensity of ROI 3)] / [(average luminous intensity of ROI 2)-(average luminous intensity of ROI 3)].

For lymphatic UCL imaging *in vivo* and Stokes emission imaging *in vivo*, 20 μ L of BDMO-doped nanoparticles were injected intradermally into the paws of female Balb/c mice (n=3). At 30 min postinjection, UCL and Stokes lymphatic imaging were performed under excitations with 730 nm laser (2 mW cm^{-2}) and 635 nm laser (2 mW cm^{-2}), respectively. For time-dependent *in vivo* imaging, after injection, images were acquired at the time points of 0.5 and 12 h, respectively. Emission light at <720 nm (UCL) and 651-671 nm (Stokes emission) were collected with the 720 short-pass filter and the band-pass filter, respectively.

For *in situ* and *ex vivo* imaging, the skin removal and lymph node harvest from mouse

were operated after *in vivo* imaging.

For signal-to-noise ratio comparison of UCL imaging *in vivo* of BDMO-doped upconversion nanoparticles and near infrared imaging *in vivo* of ICG, 20 μL of ICG (5 μM) were injected intradermally into the paws of another group female Balb/c mice (n=3). At 30 min postinjection, NIR lymphatic imaging *in vivo* of ICG was performed under excitation by 730 nm laser (2 mW cm^{-2}). Emission at 788-812 nm (NIR emission) were collected with the band-pass filter.

2. Supplementary figures and tables

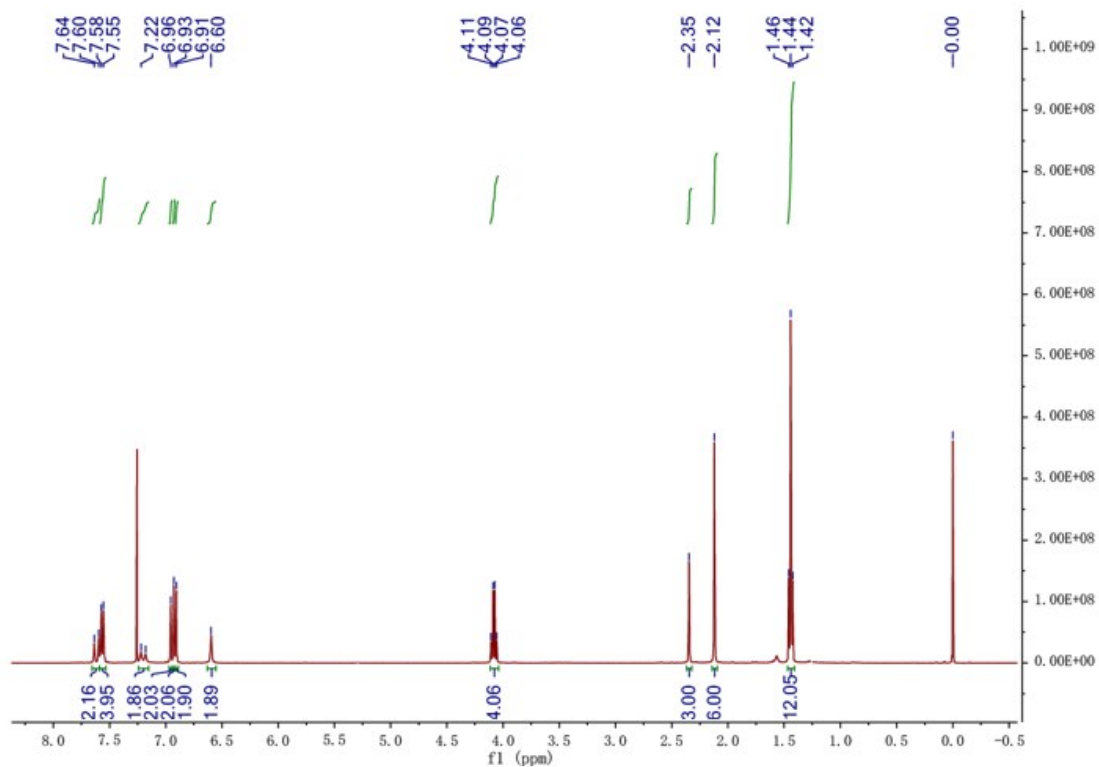


Fig. S1 The ¹H NMR spectrum of compound BDMO.

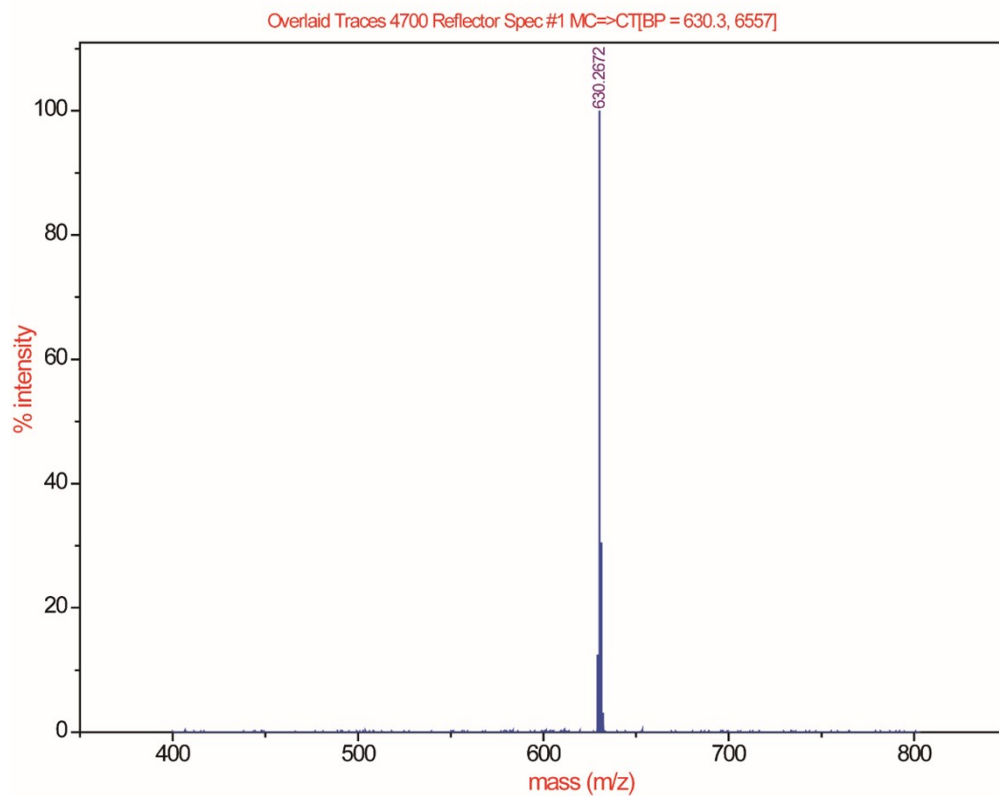


Fig. S2 The MALDI-TOF/TOF spectrum of compound BDMO.

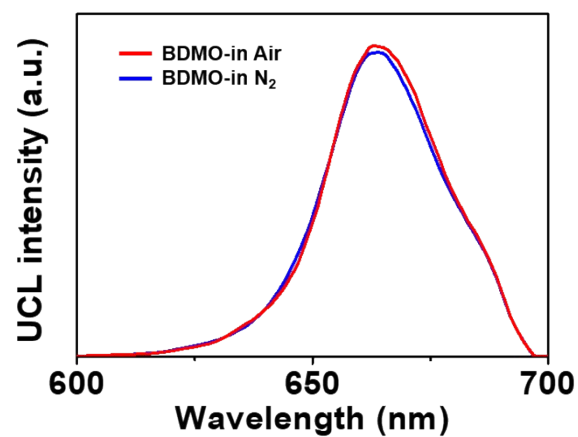


Fig. S3 The influence of oxygen on the UCL intensity of BDMO.

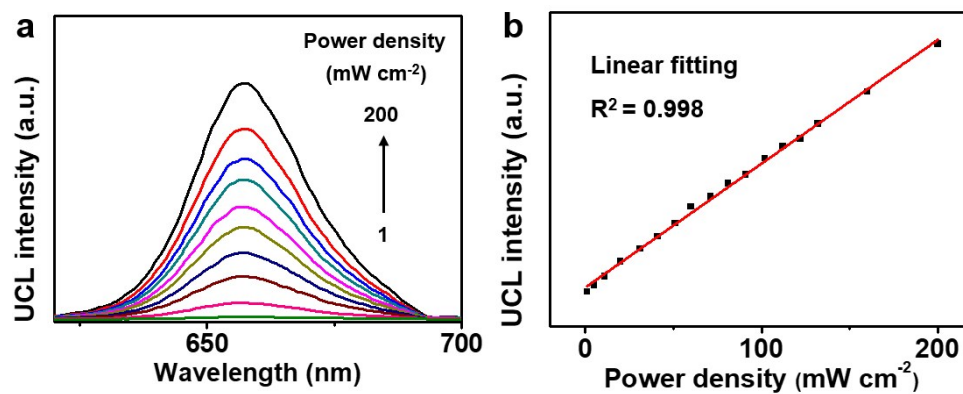


Fig. S4 (a) The UCL spectrums of BDMO ($5 \mu\text{M}$ in EtOH, $\lambda_{\text{ex}} = 730 \text{ nm}$) under different excitation power densities (1 - 200 mW cm^{-2}). (b) UCL intensity of BDMO as a function of incident power density.

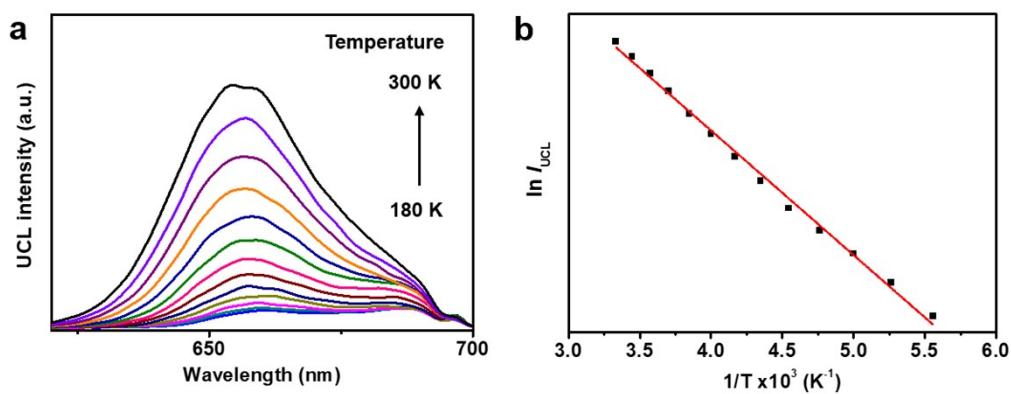


Fig. S5 (a) The UCL spectra of BDMO (5 μ M in EtOH, $\lambda_{ex} = 730$ nm) at different temperatures (180 - 300 K). (b) UCL intensity at 660 nm of BDMO as a function of temperature.

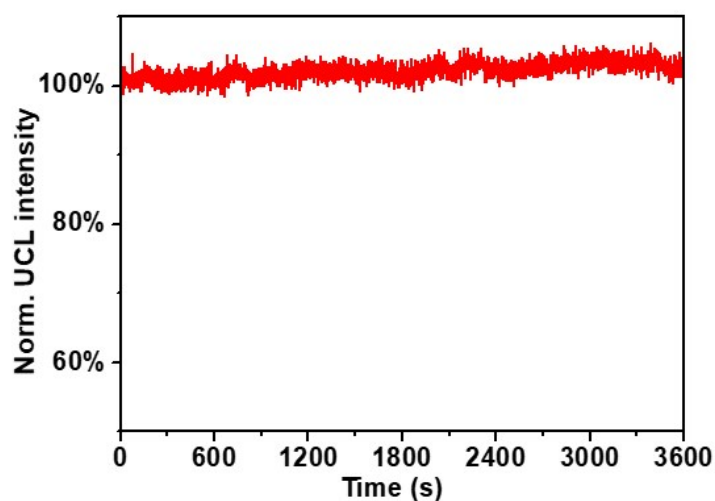


Fig. S6 The UCL intensity of BDMO (5 μ M in EtOH) under intense 730 nm excitation (1 W cm⁻²) without the removal of oxygen. **During the BDMO-based upconversion process, the UCL stability was able to maintain well in the presence of ambient oxygen.**

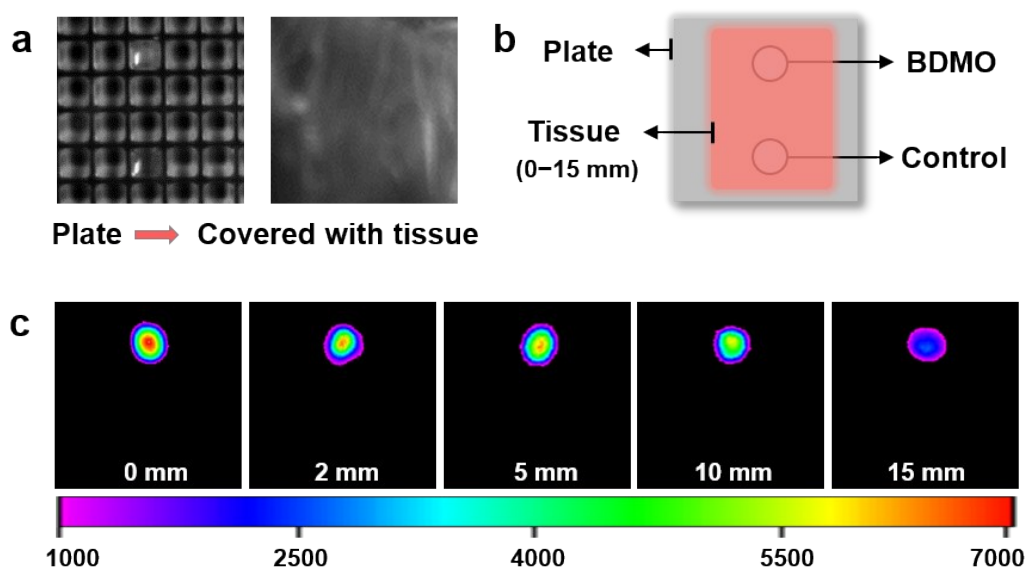


Fig. S7 (a) The bright field photos of BDMO and control group (solvent) in plate and covering with tissue. (b) The illustration of investigation experiment for tissue penetration ability of BDMO. (c) The UCL signals of BDMO passing through different thicknesses of tissues ($\lambda_{\text{ex}} = 730 \text{ nm}$). A 720 nm short-pass filter was used. **The deep-red UCL of BDMO showed high tissue penetration ability that was appropriate for potential upconversion bio-applications.**

Table S2 Crystallographic data of BDMO.

	BDMO
CCDC number	1854321
Formula	$\text{C}_{40}\text{H}_{41}\text{BF}_2\text{N}_2\text{O}_2$
Formula weight	630.56
Crystal system	orthorhombic
Space group	$\text{Pca}2_1$
A (Å)	18.394(10)
B (Å)	12.797(7)
C (Å)	14.646(8)

α (°)	90
β (°)	90
γ (°)	90
Volume (Å ³)	3447.49
Z	4
ρ_{calc} (g cm ⁻³)	1.2148

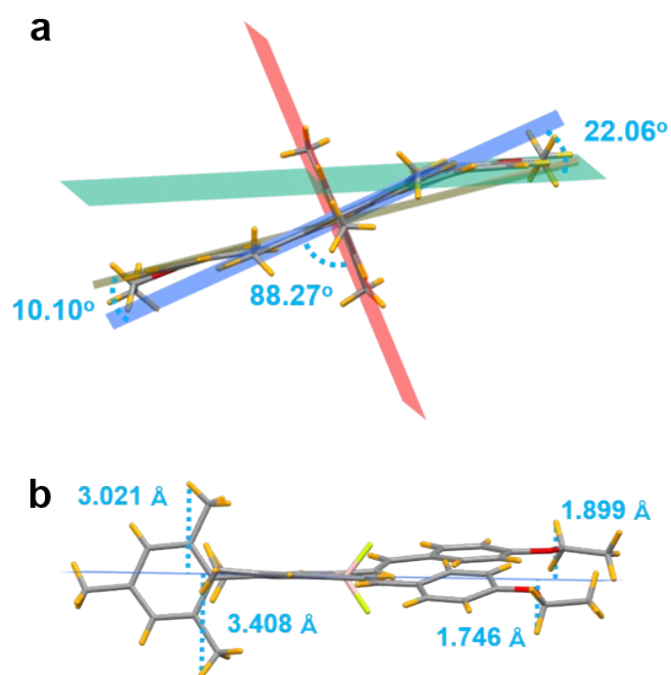


Fig. S8 (a) The dihedral angles between BODIPY core plane and meso-trimethylphenyl ring or 3,5-distyryl planes of BDMO. (b) The perpendicular distances between BODIPY core plane and meso-phenylmethyl or 3,5-distyryl groups of BDMO.

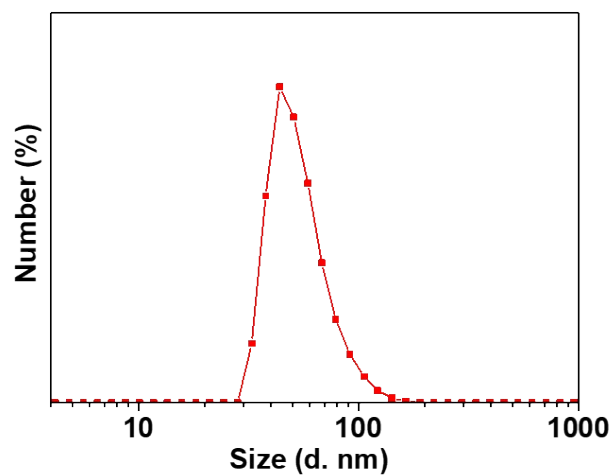


Fig. S9 DLS analysis of BDMO-doped upconversion nanoparticles at 25 °C.

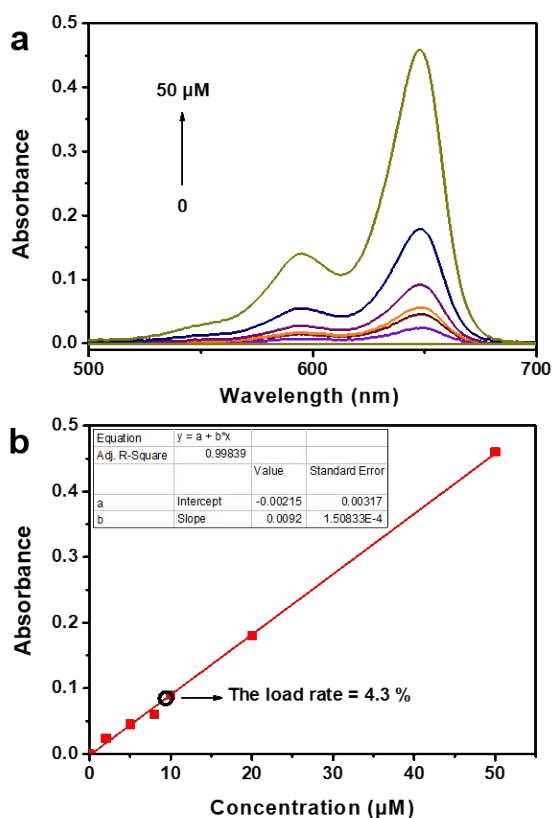


Fig. S10 (a) The absorption spectra of the BDMO in EtOH with different concentrations (0-50 μM). (b) The absorbance at 640 nm as a function of BDMO concentration. The load rate of BDMO molecules in BDMO-doped upconversion nanoparticles was determined according to this standard curve.

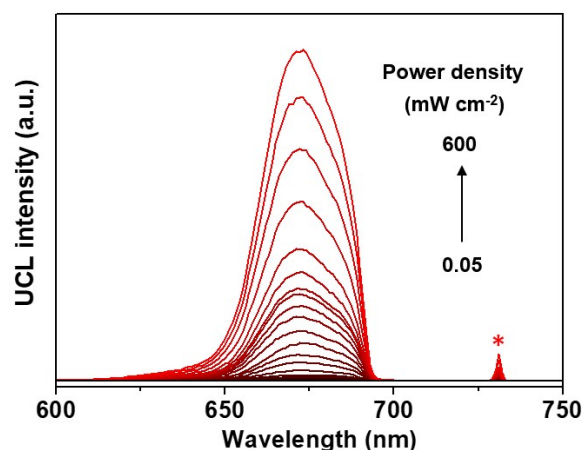


Fig. S11 The UCL spectra of BDMO-doped nanoparticles in water under different excitation power density. A 720 nm short-pass filter was used to cut-off the 730 nm excitation laser in the upconversion spectra measurement.

Table S3 The upconversion efficiency (ϕ_{UC}) comparison of different upconversion nanoparticles in literatures and in this study.

Materials	Size (nm)	Solvent	λ_{Exc} (nm)	λ_{Em} (nm)	I (mW cm ⁻²)	ϕ_{UC} (%)	Reference s
LiYbF ₄ :2%Er ³⁺ @LiYF ₄	30	Cyclohexane	980	410-690	7×10 ⁴	3.36	12
NaYF ₄ :Yb ³⁺ ,Tm ³⁺ @NaYF ₄	43	Hexane/cyclohexane/ chloroform/toluene	975	800	1.3×10 ³	~1.2	13
TTA-UC MOF	55	Water	532	445	2.5	0.64*	14
TTA-UC co-assemblies	~100	Water	515	440	1.3×10 ²	6.5*	15
TTA-UC nanomicelles	6.2	Phosphate buffered saline	532	435	~1×10 ²	~6.5	16
sTTA-UC nanoparticles	~15	Water	532	435	~1×10 ²	~7.5**	17
PtOEP/DPA-doped NPs	16	Water	532	435	5.6	1.85*	18
TTA-UC nanocapsules	95	Water	635	546	1.06×10 ²	2.4*	19
TTA PLA-mPEG NPs	33	Phosphate buffered saline	532	435	1.5×10 ²	1.9*	20

TTA-upconversion NPs	10	Water	532	433	2.6×10^2	2.25*	6
TTA-Nd-NPs	~160	Water	635	540	1×10^2	3.1	21
BDMO-doped upconversion nanoparticles	30	Water	730	660	~1	6.9	This work

*The maximum upconversion efficiency is 50% in TTA upconversion system where two lower-energy photons are annihilated to generally one higher-energy photon.

**Since the UCL of TTA-upconversion system is generated from a nonlinear process, the ϕ_{UC} reduces significantly at lower excitation power density. ϕ_{UC} increases linearly with the excitation power density up to the threshold. Above this threshold irradiance, the ϕ_{UC} saturates at a maximum value of 7.5%.

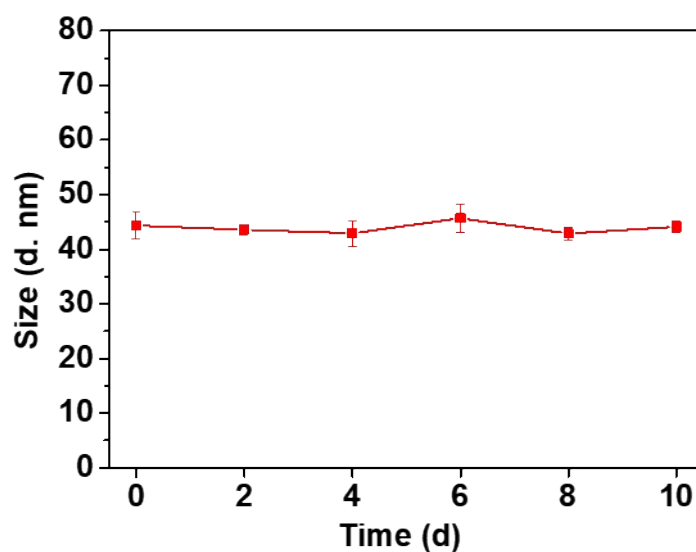


Fig. S12 DLS analysis of BDMO-doped nanopartilles in water after standing at room temperature for different time.

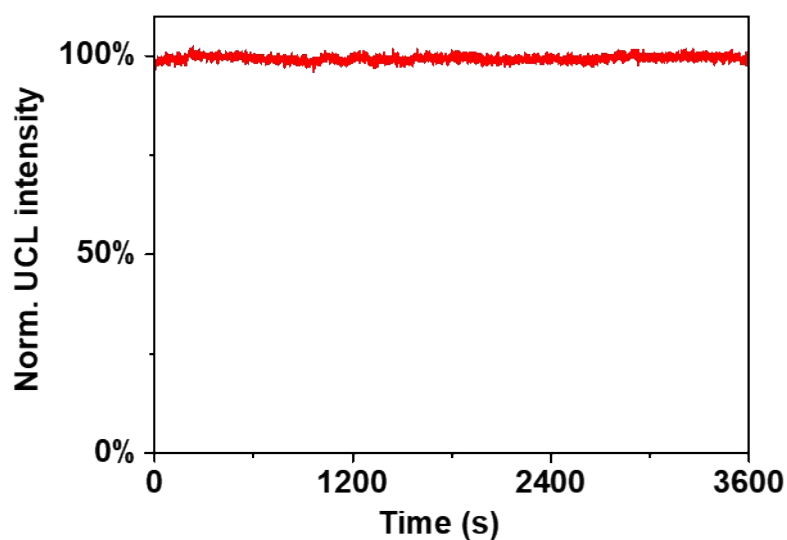


Fig. S13 The optical stability of BDMO-doped nanoparticles in water under the excitation of 730 nm laser (1 W cm^{-2}).

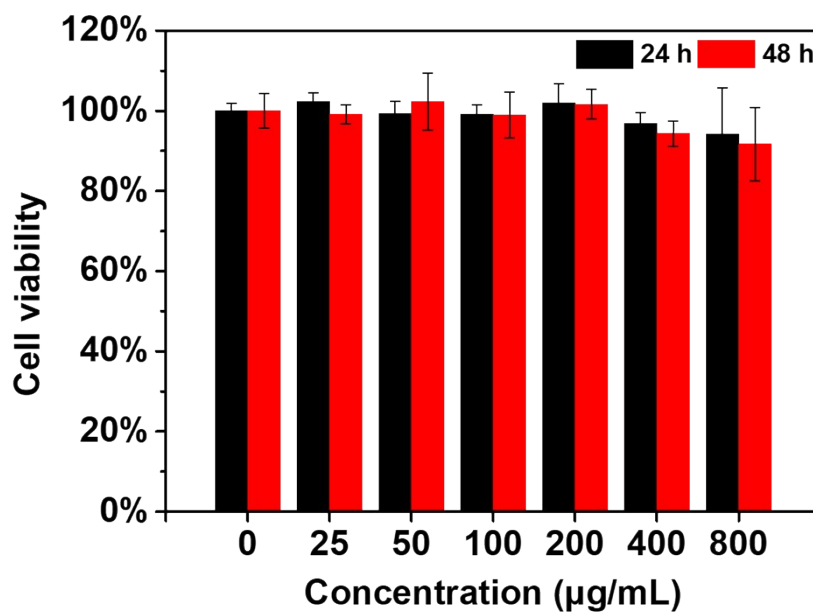


Fig. S14 Cell viability of HeLa cells incubated with the BDMO-doped upconversion nanoparticles at different concentrations for 24 and 48 h. **No obvious cytotoxicity was observed.**

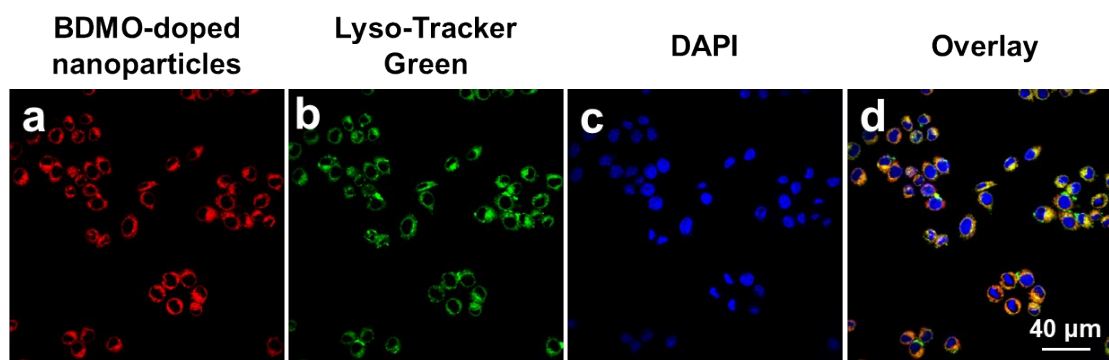


Fig. S15 Visualization of BDMO-doped nanoparticles (a) incubated with Raw 264.7 cells co-labeling with Lyso-Tracker Green (in green, b) and DAPI (in blue, c), and overlay result (d). **The intracellular images demonstrated that intense UCL signals mainly from the position of cytoplasm, which was a certain coincidence with the fluorescence signal from commercial lysosome probe. Thus, the highly efficient BDMO-doped upconversion nanoparticles has great potential for cellular imaging.**

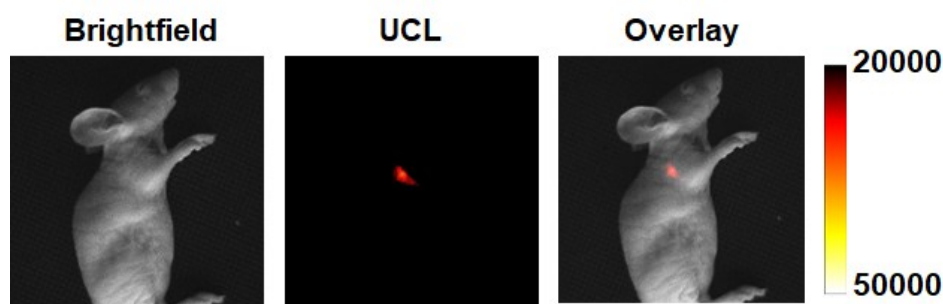


Fig. S16 Lymph node imaging of mice at 12 h postinjection of BDMO-doped upconversion nanoparticles in forepaw. **UCL signals could be still identified from SLN , which indicated that BDMO-doped upconversion nanoparticles were expected to be applied as long-term *in vivo* imaging indicator.**

3. Reference

1. L. Fu, F.-L. Jiang, D. Fortin, P. D. Harvey and Y. Liu, *Chem. Commun.*, 2011, **47**, 5503-5505.
2. A. B. Nepomnyashchii, M. Bröring, J. Ahrens and A. J. Bard, *J. Am. Chem. Soc.*, 2011, **133**, 8633-8645.
3. B.-S. Kim, D. Kashibuchi, Y.-A. Son, S.-H. Kim and S. Matsumoto, *Dyes Pigm.*, 2011, **90**, 56-64.
4. K. Benelhadj, P. Retailleau, J. Massue and G. Ulrich, *Tetrahedron Lett.*, 2016, **57**, 1976-1980.
5. N. Maindron, M. Ipuay, C. Bernhard, D. Lhenry, M. Moreau, S. Carme, A. Oudot, B. Collin, J.-M. Vrigneaud, P. Provent, F. Brunotte, F. Denat and C. Goze, *Chem.-Eur. J.*, 2016, **22**, 12670-12674.
6. Q. Liu, T. Yang, W. Feng and F. Li, *J. Am. Chem. Soc.*, 2012, **134**, 5390-5397.
7. S. Zanarini, E. Rampazzo, S. Bonacchi, R. Juris, M. Marcaccio, M. Montalti, F. Paolucci and L. Prodi, *J. Am. Chem. Soc.*, 2009, **131**, 14208-14209.
8. Y. Liu, Q. Su, X. Zou, M. Chen, W. Feng, Y. Shi and F. Li, *Chem. Commun.*, 2016, **52**, 7466-7469.
9. K. Nawara, A. Rana, P. K. Panda and J. Waluk, *Anal. Chem.*, 2018, **90**, 10139-10143.
10. M. Yu, F. Li, Z. Chen, H. Hu, C. Zhan, H. Yang and C. Huang, *Anal. Chem.*, 2009, **81**, 930-935.
11. Q. Liu, W. Feng, T. Yang, T. Yi and F. Li, *Nature Protocols*, 2013, **8**, 2033-2044.
12. Q. Zou, P. Huang, W. Zheng, W. You, R. Li, D. Tu, J. Xu and X. Chen, *Nanoscale*, 2017, **9**, 6521-6528.
13. C. T. Xu, P. Svenmarker, H. Liu, X. Wu, M. E. Messing, L. R. Wallenberg and S. Andersson-Engels, *ACS NANO*, 2012, **6**, 4788-4795.
14. J. Park, M. Xu, F. Li and H.-C. Zhou, *J. Am. Chem. Soc.*, 2018, **140**, 5493-5499.
15. H. Kouno, T. Ogawa, S. Amemori, P. Mahato, N. Yanai and N. Kimizuka, *Chem. Sci.*, 2016, **7**, 5224-5229.
16. S. Mattiello, A. Monguzzi, J. Pedrini, M. Sassi, C. Villa, Y. Torrente, R. Marotta, F. Meinardi and L. Beverina, *Adv. Funct. Mater.*, 2016, **26**, 8446-8446.

17. D. C. Thévenaz, A. Monguzzi, D. Vanhecke, R. Vadrucci, F. Meinardi, Y. C. Simon and C. Weder, *Mater. Horizons*, 2016, **3**, 602-607.
18. A. Monguzzi, M. Frigoli, C. Larpent, R. Tubino and F. Meinardi, *Adv. Funct. Mater.*, 2012, **22**, 139-143.
19. Q. Liu, B. Yin, T. Yang, Y. Yang, Z. Shen, P. Yao and F. Li, *J. Am. Chem. Soc.*, 2013, **135**.
20. W. Wang, Q. Liu, C. Zhan, A. Barhoumi, T. Yang, R. G. Wylie, P. A. Armstrong and D. S. Kohane, *Nano Lett.*, 2015, **15**, 6332-6338.
21. M. Xu, X. Zou, Q. Su, W. Yuan, C. Cao, Q. Wang, X. Zhu, W. Feng and F. Li, *Nat. Commun.*, 2018, **9**, 2698.